Polyelectrolyte composite: Hyaluronic acid mixture with DNA

I. Delač Marion, [†] D. Grgičin, [†] K. Salamon, [†] S. Bernstorff, [‡] and T. Vuletić [*,†]

Institut za fiziku, Bijenička 46, 10000 Zagreb, Croatia, and Elettra-Sincrotrone Trieste, 34149 Basovizza, Italy

E-mail: tvuletic@ifs.hr

Abstract

We studied salt-free, highly concentrated (5-200 g/L) mixtures of unfragmented (μm contour length) DNA and hyaluronic acid (HA) as a border-line example of rigid-rod/flexible-chain composite, across a broad range of concentration ratios $c_{HA}/c_{DNA} = 0.05 - 50$. By polarizing microscopy (PM) we established that the DNA and HA form clearly separated thread-like domains defined and oriented by solution shear. Within its domains DNA shows birefringent banded patterns, routinely observed for long chain mesogens. We applied small angle x-ray scattering (SAXS) to the mixtures and observed a PE correlation peak at $q^\star$ wave vector. This peak was ascribed to DNA subphase and was used as a measure of effective DNA concentration in the subphase, according to deGennes scaling relationship between the DNA mesh size $\xi = 2\pi/q^\star \approx c^{-1/2}$ and monomer concentration c. From c_{DNA} we inferred the effective c_{HA} of HA subphase, and found a proportionality $c_{HA} = 0.8 c_{DNA}$. As DNA and HA subphases are in the osmotic pressure equilibrium, HA osmotic pressure $\Pi_{HA} = \Pi_{DNA}$ is inferred,

*To whom correspondence should be addressed
†Institut za fiziku, Bijenička 46, 10000 Zagreb, Croatia
‡Elettra-Sincrotrone Trieste, 34149 Basovizza, Italy

since the DNA equation of state is known. That is, $\Pi_{HA}(c)$ scales as for the other PEs (DNA and polystyrene sulfonate, PSS), $\Pi \sim c^{9/8}$, up to about $c = 1$ M. The osmotic pressure of PEs is regulated by Manning uncondensed counterion concentrations, $c_i/c = \phi < 1$. Since HA, a weak PE due to a low linear charge, does not feature condensation, i.e. $c_i = c$, it may be used as a measure of counterion concetrations for strong PEs. Eventually, we corroborate the work by Raspaud et al.[1] who found that the concentration of counterions controlling the osmotic pressure is double the theoretical Manning-condensation defined value for DNA or PSS.

Introduction

Most biomacromolecules are polyelectrolytes (PEs) - polymers with ionizable groups on constituent monomers. PEs dissociate in polar solvents (water being the natural one) into polyions and a cloud of oppositely charged, low-molecular weight counterions. The long-range electrostatic interaction of these charged species leads to a behaviour qualitatively different than for neutral polymers[2–8] . These systems spatially arrange themselves in a way which strongly depends on the PE and added salt concentration or valence of counterions. The intrinsic rigidity of bioPEs, often higher than for the flexible neutral polymers, along with the long-range nonspecific interactions significantly affect the cellular macromolecular environment. Accordingly, there remain difficulties in understanding these systems[9–14] but there are distinctive technical applications (gene therapy, gene chips, DNA sequencing, biocompatible materials)[15–21] that can be improved with the advancements in the field of PEs. In other words, not only it is of fundamental value to understand the environment formed by PEs but this is both biologically and technologically relevant. E.g. intracellular regulatory proteins find their DNA binding sites in a crowded, strongly interacting environment of DNA and other biomacromolecules - mainly proteins[22–26] . Systems of elevated macromolecular concentration also exist on the other side of the cell wall, in the extracellular matrix - where hyaluronic acid (HA) is a prominent component[27–30] .

A region of the phase diagram of PEs at high concentrations, around 100 g/L and almost up to 1000 g/L covers the packing levels of different biopolyelectrolytes in living matter (chromosomes, viruses, amyloid particles, collagen systems)[31] . The DNA based systems have been thoroughly investigated. Different lyotropic DNA mesophases occur with the increase in effective DNA concentration[31–38] . Even at much lower concentrations bioPEs may be induced by the ionic or macromolecular environment to form structures that show local organization similar to liquid crystals. There are two distinct mechanisms. Firstly, condensation of even single PE molecules can be promoted by molecular crowding, effected by adding sufficiently high concentrations of "crowding agents" such as uncharged flexible polymers (e.g. polyethyleneglycol-PEG) or small globular proteins[26,39–42] . Secondly, condensation can occur also due to complexation with multivalent counterions or oppositely charged PEs, for DNA and for other systems, e.g. F-actin[43–50] . This latter mechanism benefits from the low-ionic strength environment where unscreened interaction with multivalent counterions leads to correlation effects that render effective attraction of two like-charged PE chains. Conversely, for the previous condensation mechanism the high ionic strength of simple salt is beneficial as the electrostatic repulsion among the PE chain links is screened - the PE domains osmotic pressure is reduced and condensation due to pressure generated by the polymer domains is facilitated. In other words, the osmotic pressure ceases to be defined by the counterions and becomes dominated by conventional, uncharged polymer depletion effects. Studies of condensation are effectively studies of the equation of state and in particular, the equation of state of DNA (osmotic pressure vs. DNA and salt concentration) is well studied with the osmotic equilibration method[1,51–53] .

The phase diagram of HA has been less extensively covered. Specifically, it's the measurements in very low added salt environment that are lacking to establish the equation of state and to produce a comparison with DNA[54–61] . PE properties of HA (a polysaccharide) render it relevant in a multitude roles in living matter. For the case here, HA is of interest as it is a semiflexible PE (structural persistence length may be up to 10 nm) more akin to

DNA (structural persistence length 50 nm) than the synthetic PEs (with -C-C- backbone, PolyStyreneSulfonate, PolyVinylsulfonicAcid, PolyAcrylicAcid: PSS, PVA, PAA, etc.) routinely used for studies of physics of polymers. The latter have the persistence length of the order of 0.25-0.5 nm. However, in opposition to DNA (or PSS), HA is a PE of a lower linear charge density, below the Manning condensation threshold [see Appendix].

Binary mixtures of two PEs are a system where both condensation mechanisms may be realised. A more straightforward case is a mixture of oppositely charged polyions. Here a rather intuitive picture is given where one of the PEs can also have a role of a multivalent counterion. A phase diagram for such a system was devised by Zhang and Skhlovskii [48] . A mixture of like-charged PEs is a system where neither of the above presented condensation scenarios applies directly [26,62–64] . That is, the crowding mechanism prefers the high-salt, highly screened environment with suppressed Coulomb interaction. A study of like-charged PEs could contribute towards further understanding of realistic, complex crowded environments [51,65–67] . For polymer mixture, there is an inherent tendency to demix because of the very small contribution from the entropy of mixing, resulting from the high molecular weight of the components. The translational entropy loss due to the phase separation is N times smaller (N=number of links in the chain) than for small molecules of similar volume fraction, while the energy gain from the contact of links is the same. This occurs even if there is no interaction (Flory parameter $\chi = 0$) between those links. Intuitively, the demixing tendencies should be stronger in the case of the repulsive Coulomb interactions between two polycationic chains like DNA and HA in a mixture - e.g. stronger than for DNA and neutral PEG. However, here we should not forget that the Coulomb repulsion is there also for the links of the same type - DNA/DNA and HA/HA. Studies of synthetic, flexible PEs have shown demixing above $5-15\%$ PE content in aqueous solution, but a non-negligible region of the phase diagram mixing does occur [68,69] .

Flory has, in a series of papers [65] investigated the statistical thermodynamics of mixtures of rodlike particles. One of the papers in the Flory series addressed the rods mixture with

coils and found that rods readily aggregate and form a subphase. The basic physical concept of Flory phase separation shows its relevance in (nano)composites [70] . That is, polymer blends with a liquid crystalline dispersed phase are of technological interest, because the LC inclusions can form a fibrillar morphology during processing, leading to a "self-reinforced" composite. While the Flory study did not include the charge effects, the relatively high persistence length of DNA and HA and other bioPEs invites this work in our consideration - bioPEs may often be regarded as rigid rods or at least as chains of jointed rods/links unlike the uncharged polymer coils. An extension of this study for the case where one of the components does cary charge, *i.e.*it's a polyelectrolyte, may be found in the works by Khokhlov and coauthors [66] and refs therein. The effect was the increase of solubility of the charged component in the bulk of the other component - *i.e.*there was some compatibility enhancement. This occurs due to the introduction of the counterions - their translational entropy loss is significant in the case of phase separation. A common experimental system of charged rods and uncharged coils is DNA mixed with PEG, used for the osmotic stress method for investigations of DNA lyotropic phases, equation of state and DNA-DNA interactions [39–42,71,72] . A system closer to the above concept of like-charged PEs is the DNA mixture with rodlike bioPE, F-actin (persistence length 10000nm). Both systems feature phase separation - DNA with PEG systems may be either single molecules assuming a compact state excluding PEG or, at higher concentrations DNA domains organize separately from PEG domains [41,46] . The F-actin/DNA system with di- and tri-valent counterions was shown to phase-separate towards formation of F-actin bundles and DNA toroids [63] . F-actin was also shown to form nematic phases when mixed with DNA in pure water or in up to 10 mM monovalent salt conditions [64] . Interestingly, in the latter case the DNA functioned as the osmotic stressing agent, as e.g. BSA (bovine serum albumin) for DNA [26] .

We present here a study of DNA and HA mixture with nominal DNA and/or HA concentrations covering the range 0-100 g/L. Firstly, our study is another take in this interplay of chain rigidity and charge density of chains in the mixture. That is, HA is the flexible

component here and it carries a weaker charge than DNA. However, it is not uncharged as PEG and it is quite closer in rigidity to DNA than DNA is to F-actin or to PEG. In brief, F-actin/DNA, DNA/HA and DNA/PEG are three characteristic cases from a spectrum of possible semirigid PE mixtures. The essence of all these concepts, both theoretical and experimental was that a system of two PEs of rather different rigidity was studied. The more rigid component will form the ordered phase. Our study checks for this. By polarizing microscopy (PM) we have observed birefringent, microns thick, elongated domains appearing in DNA+HA samples of nominal DNA concentration of only 10 g/L - below the concentration for formation of anisotropic DNA phase. In coexistence were optically isotropic HA domains of similar elongated shapes. HA solutions are not known to show birefringence at any concentration. On the other hand, DNA shows anisotropic organization visible by PM already above 10 g/L[37,38] . However, while we do attempt to quantitate the fraction of HA and DNA from the area of their respective domains this still is not a very precise method. We managed to infer from SAXS data that the phase separation is complete and that there is no mixing of DNA and HA within domains. We base this also on our recent SAXS study of DNA and HA solutions in very low added salt[73] . Others have shown[74] and we have checked that the DNA features a well defined scattering maximum (polyelectrolyte peak) that depends on the square-root of the concentration. Importantly, this is a rather precise and reproducible feature (see Supporting Information). However, scattering from the HA system is significantly less intense and reveals, instead of a scattering maximum, only a weak shoulder but with a similar concentration dependence. Thus we found that, for DNA/HA mixture the position of the scattering peak is a direct measure of DNA local concentration (concentration within the DNA domains) in the range of 2-200 g/L and beyond. This then provides the volume taken by DNA subdomains and finally provides the volume taken by HA domains and the effective HA concentration within those domains.

Secondly, we study here the DNA/HA mixture without the added salt. Thus it's the counterions that regulate the osmotic pressure in this system. Our precise knowledge of

DNA and HA effective concentrations allows us to infer osmotic pressure vs. monomer concentration for HA from the one for DNA. We find that for HA, as for DNA there is a scaling[75] $\Pi \propto c^{9/8}$. This scaling is valid up to 400-500 mM (monomers). We find an agreement also with the result for the flexible PE polystyrene sulfonate (PSS). Our result for HA complements the previously available results on osmotic pressure of HA in a monovalent salt environment.

Finally, it is of additional interest that DNA is a highly charged polyelectrolyte that features Manning condensation while HA is below the Manning limit of one elementary charge per Bjerrum length (see Appendix). As noted by Raspaud et al., [1] for DNA in low salt conditions the fraction of the counterions that contribute to osmotic pressure (detected by osmometry) may be double the fraction of Manning free counterions given by both Manning theory and the experimental studies that corroborate the theory. With HA, there is no condensation, so the number of counterions that define the osmotic pressure is clearly defined and our data appear to be precise enough to corroborate the result by Raspaud. In other words, the counterion concentrations of HA may serve as a reference for the DNA counterion concentration.

Experimental

Materials

Solutions and mixtures of deoxyribonucleic acid (DNA) and hyaluronic acid (HA) solutions, both in the form of sodium salts, were prepared with ultrapure water (Millipore Milli-Q), without addition of any simple salts. Dissolving without a buffer leads to a solution where the pH is defined by the CO_2 dissolved in water, which leads to a pH of about 6, with both DNA (pKa = 0) and HA (pKa = 3.2[60]) fully ionized. In our previous studies[73,76–79] we used the DNA and HA samples described below, and ascertained that the salt content in these samples is negligible, less than one added salt ion per 10 monomers. As such, samples

dissolved in ultrapure water are taken to be free of added salt.

For DNA samples we used Salmon testes lyophilized DNA obtained from Sigma-Aldrich (Cat. No. D1626) which is polydisperse, with chain lengths in the range from 2 kbp to 20 kbp or higher (contour length 0.7-7 μm). For HA we used HA from Streptococcus equi sp. from Sigma-Aldrich (Cat. No. Fluka53747) with an average polymerization degree of 4000 (contour length of 4 μm) and a polydispersity index 1.3. For both, the low protein content is declared by the manufacturer. Since they have rather long chain lengths, the corresponding dilute-semidilute crossover concentrations are expected to be several orders of magnitude below the concentration range studied [80,81] so we conclude that our samples are in the semidilute regime.

We had two sets of samples prepared according to the following protocols (concentrations are given as dry mass per total volume of the sample):

Protocol I - for SAXS and polarizing microscopy (PM). We prepared mother solutions of DNA with concentrations 5-80 g/L by adding a given amount of dry DNA fibers (5-80 mg) and ultrapure water (1 mL) into a small polyethylene bag each. During the course of the experiment, more and more dry HA grains were being added to these bags, thus resulting in an increasing HA concentration in the binary DNA/HA mixture, at a fixed DNA concentration. The maximum HA added was about 100 mg per 1 mL DNA solution (10% by volume) and dissolving HA could not have swollen the total volume more than a couple of percent beyond 1 mL. For the purpose of our analysis, the consequent deviation in DNA concetration is negligible. The range of both polyelectrolyte concentrations is shown in 1. The preparation procedure for each consecutive HA concentration was the following: first, a small cut was made in a bag with the mother solution and a couple of μL of sample was extracted from the plastic bag (in a manner toothpaste is squeezed out) and onto either the SAXS sample holder or onto a glass slide for PM. The bag was weighed to establish the amount of sample extracted. While the measurement was conducted on the previous sample, dry HA was added to the bag with the solution, the bag was sealed (welded) and weighed

as a control of the added mass. Bag was then squished between fingers for several minutes to ensure complete dissolution of HA and thorough mixing of the contents. A next sample (now with the next higher HA concentration) was then extracted and applied in the same manner like the previous one thus completing the cycle. This was done up to about 100 g/L of HA, for each of the DNA solutions.

Protocol II - for SAXS. We prepared mother solutions of both DNA (C_{DNA} =200g/L) and HA (C_{HA}=40g/L). These were then mixed in 10% steps (90:10, 80:20, ... , 10:90) which resulted in 9 (+2 mother solutions) different solutions across the range from pure DNA to pure HA. We emphasize that, unlike the protocol I where HA grains were mixed into the solution, here we mixed two solutions which were allowed to equilibrate for a month. Nevertheless, no qualitative or quantitative difference in properties was observed for these samples when compared to protocol I (see later Figure 7). The DNA mother solution C_{DNA} from this set was also used for establishing the dependence of the polyelectrolyte correlation peak observed in SAXS vs. DNA concentration. (see supporting information)

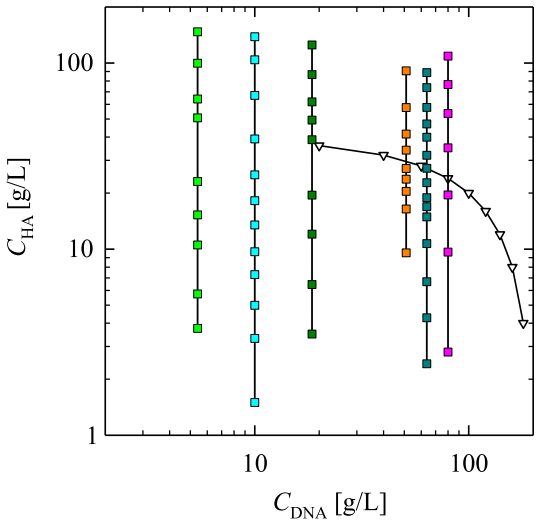

Figure 1: Mass concentrations of DNA and HA in the binary mixtures prepared by Protocol I (circles) and Protocol II (triangles). Vertical lines denote different DNA mother solutions that have been gradually complemented with HA.

Methods

Small-angle X-ray scattering

The SAXS measurements have been carried out at the high-flux SAXS beamline at the ELETTRA synchrotron light source (Trieste, Italy). [82] The scattering patterns were recorded with a 2D image plate detector (Mar300, MarResearch, Norderstedt, Germany) positioned at the distance $L = 1.32$m from the sample. The detector covered the q-range ($q = 4\pi(\sin\theta)/\lambda$, where $\lambda = 1.54$Å is the wavelength and 2θ is the scattering angle) of interest from $q_{min} = 0.16$ nm^{-1} to $q_{max} = 5.9$ nm^{-1}. The angular calibration of the detector was performed with silver behenate powder (d-spacing of 58.4 Å). The X-ray beam size at the sample position was set to 0.5×3.0mm^2 (V x H).

The sample solutions were measured either in quartz glass capillaries with a diameter of 1 mm or in a specially designed gel-sample-holder, enclosed between two layers of mylar, depending on the sample solution viscosity. The measurements were performed at 25°C .

Care was taken that no radiation damage was affecting the samples. This was done by recording multiple short frames (10 sec each) on the same sample volume of several DNA (20, 40 and 60 g/L), HA (10, 20, and 30 g/L) and some binary DNA/HA mixtures, thereby ascertaining the maximum acquisition time during which no change of the scattering pattern occurred. For all solutions which contain DNA, a decrease of scattered intensity was observed after the 8^{th} frame, while for pure HA solutions the scattering intensity was persistent even after the 60^{th} frame. This finding indicates that some DNA chain degradation occurs, likely induced by the high flux of the beam. Thus, we selected 60 sec as an exposure time for measuring the radiation scattered by the samples.

Before the analysis, the 2D-images were corrected for the detector response and the background scattering (pure H_20) was subtracted. From each 2D-image, 1D scattering profiles (curves) at several azimuths were extracted in order to quantitatively analyse scattering spectra for each DNA/HA mixture.

Polarization Microscopy

Polarizing microscopy (PLM) observations were done between a slide and coverslip. To prevent dehydration, the preparations were sealed by epoxy. The thickness of the preparations was ranging from 50 μm to 200μm. We used an Optika N-400 POL polarizing microscope with Optikam B5 digital camera. A quartz first order retardation plate (λ-plate) was inserted at 45° between crossed polars to analyze the orientations of molecules in particular domains.

Results

Phase separation

Polarizing microscopy offers an immediate insight in the nature of the mixture of DNA and HA. That is, we remind that well defined mesophases are routinely formed with fragmented, monodisperse DNA, s.c. nucleosomal DNA. These fragments are around 50 nm or 150 bp and feature cholesteric patterns above 100-150 g/L and columnar hexagonal above 300 g/L [36] . Long (in μm), unfragmented DNA strands in solution may align in parallel and present birefringent textures in polarizing microscopy. Long DNA does not reach liquid crystaline phases like fragmented DNA, but the ordering starts at quite lower concetrations, below 20 g/L[37,38] . On the other hand, HA is not known to show supramolecular organisation that could be detected due to its birefringence. A principal birefringent texture for long polymers are s.c. banded patterns. Banded patterns form for DNA but also for other polymers, e.g. xanthan (a polysaccharide but a helical, chiral molecule) ([33] and refs. therein). In DNA solutions, these patterns occur without a defined boundary between isotropic and birefringent regions of the sample. This is unlike e.g. cholesteric droplets, formed by shorter mesogenic molecules, which are well defined against isotropic background.

Our PLM images of DNA/HA mixtures consistently show coexistence of nonbirefringent

and birefringent domains. In Figure 2. we show PLM images from a mixture of 49 g/L DNA and 18 g/L HA that have been left to equilibrate for 6 months (sealed between a slide and a coverslip). Images are taken with a λ plate (full wave retardation plate) inserted in the optical path between the crossed polars, after the sample. This allows determination of the orientation of macromolecules. Dashed lines in the images denote the general orientation of macromolecules in a large rope-like domain that contains many aligned strands. When the rope is parallel to the fast axis of the λ-plate (Figure 2a) it is coloured yellow/orange (as negatively birefringent DNA should be) and when perpendicular (90° rotated sample, Figure 2c) the rope turns blue. At 45° (mid panel, Figure 2b) it is almost extinguished. Optically isotropic (nonbirefringent) domains are consistenly red/magenta tinted independent of the sample rotation. The appearance of the mixture is directly reminiscent of unfragmented DNA mixture with neutral, flexible polymer like polyethylene glycol (PEG)[36] - in the mixture, DNA and PEG remain in separated domains. PEG is routinely used to induce DNA condensation and mesophase formation, and here, presumably HA takes this role. This is our first indication that the isotropic domains do not contain DNA, but only HA. Even if isotropic, HA domains did contain some DNA, its concentration must be below 10 g/L, otherwise the domains would show some birefringence.

In Figure 3 the banded pattern region from Figure 2a (rectangle) is enlarged. Banded patterns are distinct from apparently similar cholesteric textures in the manner that the relative thickness of the bands (of different coloring) changes upon rotation of the sample. Between Figure 2a and c, blue or yellow bands dominate for different orientations. In the present preparation the banded pattern is formed at the end of the highly aligned rope when the molecules from the rope fan and expand between two isotropic domains. On the right hand side the strands are undulating, change local orientation periodically - which leads to appearance of the bands, as denoted by the schematics in the image. On the left hand side the strands are extended along the neighboring isotropic domain and no bands are visible.

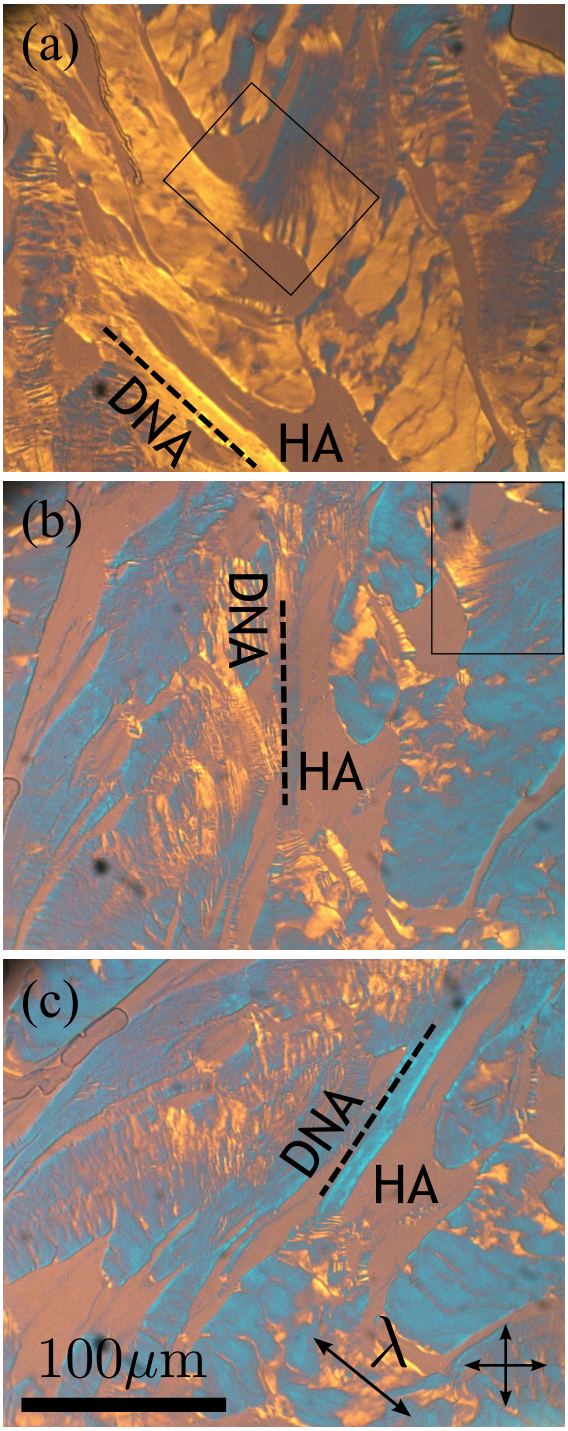

Figure 2: Polarizing microscopy (PLM) images taken with λ-plate inserted, of DNA 49 g/L + 18 g/L HA mixtures. Birefringent, presumably DNA domains are orange or blue, while nonbirefringent, presumably HA domains are red. Dashed line denotes the orientation of negatively birefringent DNA molecules, highly aligned in a rope. The rope appears orange when the chains are parallel to the λ-plate fast axis (λ-arrow), blue when perpendicular and extinguish when at 45°. Crossed arrows denote the orientation of the crossed polars. Rectangles denote the area enlarged in Figure 3.

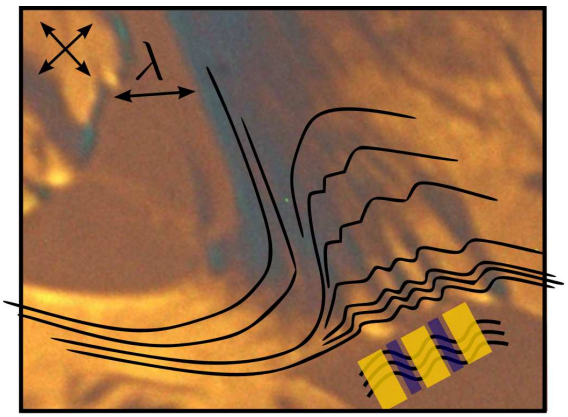

Figure 3: Enlarged area from Figure 2a presents banded patterns typical of long polymers. Upon 45° rotation, local orientation of the undulating DNA strands in relation to λ-plate axis (λ-arrow) changes as does the coloring of the bands. Lines represent the orientation of DNA molecules. Crossed arrows denote the orientation of the crossed polars.

Solution anisotropy

Figure 4 shows a series of 2D SAXS patterns for DNA/HA samples at various additions of HA and grouped by DNA mass concentration, C_{DNA}: 17 g/L, 49 g/L and 65 g/L in the first, second and third column, respectively. The main feature observed for all of the measured DNA/HA binary solutions is the appearance of the ring-like scattering maximum, indicating the existence of a short-range ordered structure in the solutions. As PE chains are negatively charged, the repulsive interaction between them produces a short-range ordered mesh which is revealed in SAXS experiments through a more or less intense scattering maximum at $q^{\star}$. We know from our recent work[73] (as well from other works[57,59]) that the pure HA solutions show only a relatively weak and wide shoulder in scattering intensities, unlike the DNA solutions. There is a reason for that: the sugar groups located on the HA chain lack the scattering power of relatively heavy P atoms present in the phosphate groups of a DNA chain. DNA also retains in its vicinity relatively heavier Na^{+} counterions,[13] unlike HA (which features no Manning condensation - see Appendix). The absence of a clear scattering maximum is also a consequence of the more disordered mesh due to the weaker electrostatic interaction between HA chains that are of lower linear charge density. Thus, for DNA/HA binary mixtures the signal should be dominated by the DNA macroion partial scattering

function. Taking into account the lack of a clear maximum for pure HA solutions, we can conclude that the appearance of the scattering maximum in the SAXS spectra for DNA/HA solutions visible in Figure 4 has its origin in the DNA inter-chain arrangement.

For DNA sample C_{DNA}=17 g/L without HA addition (first column, first row in Figure 4), the SAXS ring is isotropic in intensity distribution. By adding HA in this DNA mother solution (down the columns in Figure 4), as well as with the increase of DNA concentration for HA free samples (along the first row in Figure 4), one may notice that the azimuthal intensity distribution at the peak position of the ring becomes anisotropic. The anisotropy in scattering has two-fold symmetry which indicates a preferential orientation of the DNA macroions, at least across the scattering volume ($0.5\times0.5\times3$mm). Moreover, the appearance of anisotropy in SAXS correlates with the appearance of birefringence due to the alignment of DNA strands in the sample. For example, C_{DNA}=17 g/L DNA without HA is nonbirefringent in PLM and isotropic in SAXS, while C_{DNA}=17 g/L DNA with C_{HA}=12 g/L HA shows a weak birefringence that occurs across a large portion of the preparation between the slide and coverslip and is anisotropic in SAXS (second row, first image in Figure 4) One may check also the Supp. Info for comparison of PLM images of C_{DNA}=49 g/L DNA with HA contents C_{HA}=18 g/L, 42 g/L and 87 g/L with the respective SAXS patterns presented in Figure 4 - central column. Our DNA/HA mixture shows (see Figure 2) isolated and rope-like birefringent domains formed from aligned DNA strands. A typical length of these domains is of the order of 100 μm. This means that the scattering volume contains of the order of $10^2 - 10^3$ domains which should be, in principle, randomly oriented and produce isotropic SAXS patterns. However, we believe that DNA domains acquire a preferential direction during insertion of DNA/HA mixture into the SAXS sample holder. Namely, as most of the DNA/HA mixtures are viscous, they were inserted into SAXS sample holder by squeezing them out from the small hole made on the corner of plastic bag wherein they have been prepared and mixed. Thus, the sample was under shear and flow and the domains reoriented themselves along[59,83] - eventually producing the anisotropy in SAXS patterns.

Interestingly enough, upon further increase in HA concentration, the SAXS anisotropy gradually disappears (last two rows in Figure 4). We may only speculate that this is the effect of the increased viscosity which prevents the alignment of DNA into any larger (ropelike) domains - there is simply not enough time for these to form during the sample flow.

Compression of DNA subphase upon HA addition

A feature more relevant to this work, visible in Figure 4 is the increase of the ring radius ($q^\star$) as C_{HA} increases. We illustrate this better using 1D SAXS spectra shown in Figure 5 for C_{DNA}=10 g/L solution with an increasing HA content. Importantly, the increase in $q^\star$ with the increase in HA reflects the decrease of the mean DNA interchain separation. In other words, the DNA subphase is compressed upon HA addition.

The evolution of $q^\star$ as a function of the monomer concentration ratio of the two PEs, $c_{\mathrm{HA}}/c_{\mathrm{DNA}}$, is presented in Figure 6. We have studied six different DNA initial concentrations and the results in the Figure 6 show how the SAXS peaks shift upon addition of HA in comparison to HA-free DNA solutions (the smaller points on the left axis). Our manner of presentation and the results shown in Figure 6 are qualitatively similar to the study of F-actin/DNA mixtures by Lai et al.[64] (see Figure 3c. there). In their work, the scatterer is F-actin, the more rigid and more ordered mixture component, while DNA chains are the flexible, weakly scattering component that lacks ordering. The effective role of DNA chains is switched in DNA/HA mixture where now DNA is the more rigid, mesogenic, birefringent and strongly scattering entity. For both systems, F-actin/DNA and DNA/HA here, $q^\star$ shifts up with an increase in the monomer concentration ratio of the two PEs, in our case even for very small amount of HA added - $c_{\mathrm{HA}}/c_{\mathrm{DNA}} \approx 0.1$. Lai et al. emphasize a power law dependence of $q^\star$ on the ratio $c_{\mathrm{DNA}}/c_{\text{F-actin}}$. They find this for a rather narrow range of monomer concentration ratios from 1-6. In a similarly limited range of ratios, $1 < c_{\mathrm{HA}}/c_{\mathrm{DNA}} < 10$, we also find the same power law dependence. However, for the much lower $c_{\mathrm{HA}}/c_{\mathrm{DNA}}$ ratios that we cover in our study, this dependence necessarily vanishes, as the $q^\star$ value approaches

the $q_0^\star$ value for DNA alone (points on the Y-axis in Figure 6 and see also the Supp. Info. Fig.1). Empirically, the $q^\star$ dependence is given by

$$q^\star = q_0^\star \sqrt{1 + \Gamma c_{\mathrm{HA}}/c_{\mathrm{DNA}}} \tag{1}$$

as denoted in Figure 6. The square-root dependence stems from the fact that $q^\star$ reflects the mesh size which scales with the square-root of the concentration (Supp. Info. Fig.1).

It is also noteworthy that the SAXS intensity ring is clear and relatively strong which indicates that, although in the DNA/HA solutions exist many separated DNA domains, all of them feature a similar characteristic length scale (see Supp. Info. for the comparation of FWHM of the scattering peaks at each $q^\star$ presented in Figure 6 and FWHM of the scattering peaks for the DNA solutions without HA).

Discussion

A complete phase separation?

From the above we may conclude that we never observed a single phase HA/DNA mixture, for a rather broad range of mixture ratios (0.05-30) and total PE content 0.5-25%. That is, our SAXS data indicate that even the smallest amounts of HA added to the mixture were always to occupy a separate volume, and reduce the volume available to DNA. This reflects the fact that the SAXS correlation peak of the mixture is always shifted upwards in comparison to pure DNA (see Figure 6). These shifts can occur only if the DNA concentration increases upon HA addition. If HA completely intermixed with DNA and formed a single phase, then the latter would still occupy the same volume. In that case the DNA concentration would not change - and the SAXS peak would not shift - contrary to our observation. Interestingly, mixing of the like charged (synthetic) polyelectrolytes and formation of a single phase has been found up to 5-15% of total PE content in water, *i.e.*50-150 g/L[69] - from SAXS, our

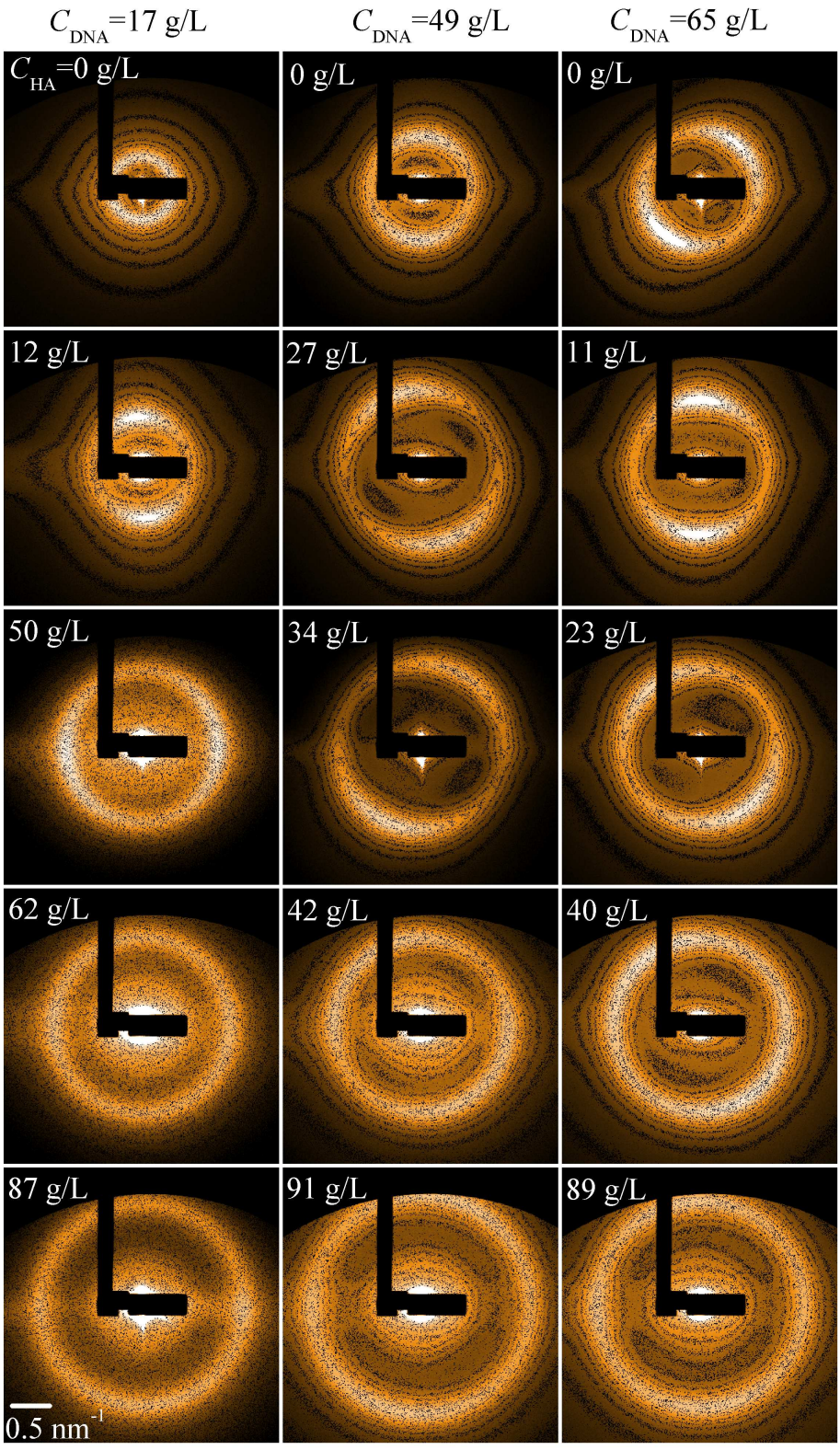

Figure 4: selected 2D-SAXS patterns for three different fixed nominal DNA concentrations - for each column and with different amount of HA added - in rows.

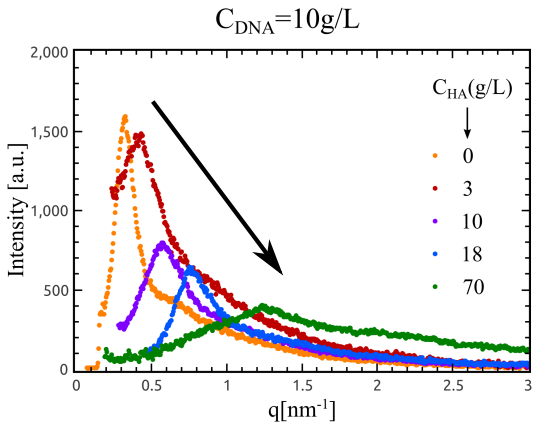

Figure 5: 1D-SAXS spectra of DNA/HA binary mixtures for C_{DNA}=10 g/L with varying concentration of HA up to C_{HA} =70 g/L. The increase in HA content shifts the scattering maximum $q^{\star}$ to higher values.

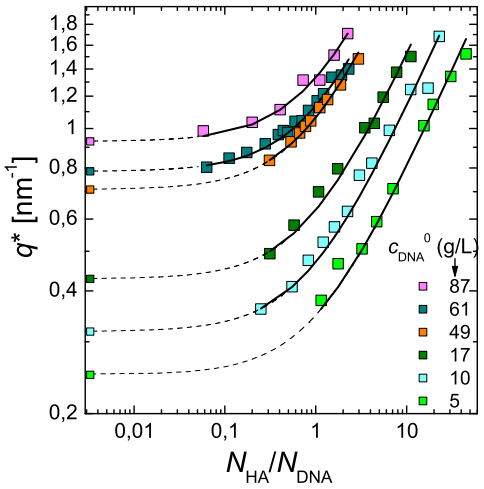

Figure 6: SAXS peak positions $q^{\star}$ shift up from the values for pure DNA mother solutions (points on the left Y-axis) upon addition of HA (shown as the increase in $c_{\mathrm{HA}}/c_{\mathrm{DNA}}$).For higher $c_{\mathrm{HA}}/c_{\mathrm{DNA}}$ ratios the peaks shift according to a power law $q^{\star} \sim (c_{HA}/c_{DNA})^{1/2}$.

DNA/HA mixtures appear quite separated even at 1% total PE content.

In accordance, polarizing microscopy (PLM) demonstrates the existence of separated phases - but it's not applicable in the low DNA/HA concentration range as 17 g/L (2% or lower) DNA solutions are not birefringent. Also, PLM does not tell on the possibility that some HA is mixed into DNA domains - it's a plausible scenario that we need to investigate further. In the opposite case, if DNA intermixed into HA domains would render these optically anisotropic - and we do observe the isotropic domains. Anyhow, PLM is not quantitative - only provides qualitative information. In the following we will analyse our data further by proposing a scenario where some HA mixes into DNA phase. As for the reasons just above , as well as for simplicity we do not consider the opposite, that some DNA mixes into the HA subphase.

We base the analysis on our experimental result that the SAXS peak originates from DNA subphase. In our recent paper,[73] we showed for DNA solutions across two decades in concentration from 2-200 g/L that - as expected in the framework of the scaling theory[6] - the relationship between $q^\star$ and concentration is precisely

$$q^\star = 2\pi(b_{\mathrm{DNA}} n_{\mathrm{DNA}})^{1/2} \tag{2}$$

where b_{DNA}=0.34 nm is the DNA monomer size and n_{DNA} is the monomer(basepair) number concentration (see also Supp. Info.). Wang & Bloomfield[74] obtained before the same equation, although for the nucleosomal DNA 146bp fragments. For these the studied concentration range was mainly below the liquid crystalline ordering concentration, unlike ours which starts to show limited ordering amidst the studied range. Nevertheless, no shift is discernible in $q^\star$, or a change in slope away from 0.50 in our data within the experimental error. That is, the position of the scattering maximum $q^\star$ is a variable, which in the isotropic solution may be regarded as the measure of the characteristic length scale $\xi_{\mathrm{DNA}} \sim 1/q^\star$ of an isotropic, random DNA mesh and upon alignment of DNA chains and precholesteric textures formation as an average distance $L_{\mathrm{DNA}} \sim 1/q^\star$ between parallel chains. These two

parameters are quite close in value and thus the $q^\star$ vs. c dependence is unaffected by this qualitative change. One may read from Eq. 2 that the value of $q^\star$ is simply given by the total (contour) length of all DNA macroions constrained in a volume allocated to the DNA molecules. We found[73] that the equation holds for the weakly charged, however rather rigid HA, while Combet et. al.[84] found that corrections are necessary for various flexible PEs.

Now, we start by assuming a completely separated DNA and HA phases and we denote coresponding volumes as $V^\star_{\rm DNA}$ and $V^\star_{\rm HA}$, where the total sample volume is $V = V^\star_{\rm DNA} + V^\star_{\rm HA}$. When we normalize to V we get $1 = V^\star_{\rm DNA}/V + V^\star_{\rm HA}/V$. This relationship may be expressed also with the effective concentrations of DNA and HA ($c^\star_{\rm DNA}$, $c^\star_{\rm HA}$, monomolar concentration) in those subphase volumes and by the nominal monomer concentrations $c_{\rm DNA}$ and $c_{\rm HA}$ (defined across the total volume - converted from the mass concentrations in Figure 1):

$$1 = c_{\rm DNA}/c^\star_{\rm DNA} + c_{\rm HA}/c^\star_{\rm HA} \tag{3}$$

Here we note that all the variables are experimentally accessible except $c^\star_{HA}$, thus:

$$c^\star_{HA} = c_{HA}/(1 - c_{DNA}/c^\star_{DNA}) \tag{4}$$

Using this expression and our SAXS length scale calibration expression ($\sqrt{(}c^\star_{DNA}) \sim (2\pi/q^\star)$) we convert all the $q^\star$ data points for different DNA concentrations from Figure 6 to get the corresponding $c^\star_{DNA}$ values necessary for obtaining the $c^\star_{HA}$ value.

Interestingly, if we plot these data as $c^\star_{HA}$ vs. $c^\star_{DNA}$ (see Figure 7) we get a simple linear relationship

$$c^\star_{HA} = \Gamma \times c^\star_{DNA} \tag{5}$$

where $\Gamma = 0.85 \pm 0.04$

The above result is directly related to the empirical relationship we presented before.

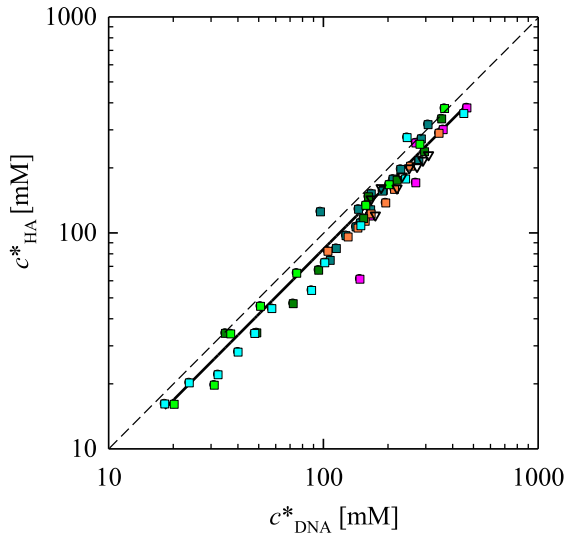

Figure 7: Effective concentration of HA vs. the effective concentration of DNA is shown for the binary mixtures prepared by Protocol I (circles) and Protocol II (triangles). The effective concentration of DNA is calculated from the experimentally obtained $q^\star$ measured for a given mixture (see Figure 1). The nominal concentrations of DNA and HA that define a mixture, as well as $c^\star_{DNA}$ enter the expression for calculation of $c^\star_{HA}$.

That is, if we rewrite Eq.3 by inserting Eq.5 we get

$$c^\star_{\mathrm{DNA}} = c_{\mathrm{DNA}}(1 + \Gamma \frac{c_{\mathrm{HA}}}{c_{\mathrm{DNA}}}) \tag{6}$$

which is analogous to Eq.1, if we take into consideration that $q^\star \sim \sqrt{c^\star_{\mathrm{DNA}}}$ and $q^\star_0 \sim \sqrt{c_{\mathrm{DNA}}}$. If the effective concentration ratio Eq.5 is converted to a ratio of the characteristic length scales (mesh size) of two separated phases, DNA and HA, we obtain that $\xi_{\mathrm{HA}} = 0.62\xi_{\mathrm{DNA}}$. In other words, in the mixture, the HA mesh size is proportionally smaller than the DNA mesh size.

With the above relationships a (pseudo)ternary phase diagram (Figure 8a) may be constructed for the DNA/HA mixture, in analogy to the work on synthetic, like-charged PE mixtures by Hellebust et al.[69] The nominal concentrations of c_{DNA} and c_{HA} are the initial (gravimetrically determined) concentrations presented by mid-points of the tie-lines. The tie-lines connect the end points found at the edges of the triangular diagram. One end-point denotes the concentration of the DNA subphase (where HA is zero due to inmiscibility

constraint) and the other of the HA subphase (where DNA is zero).

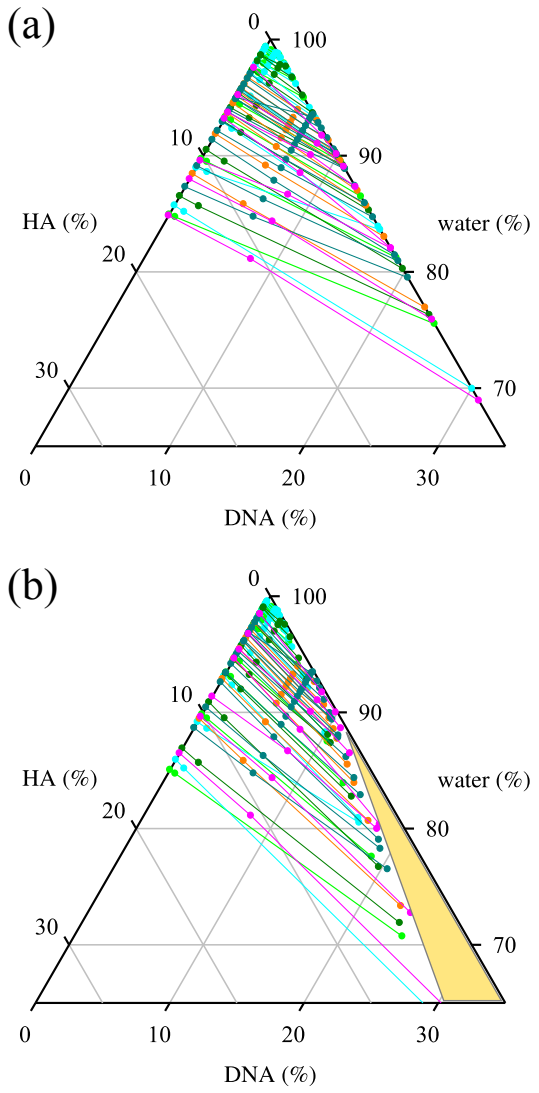

Figure 8: (a)Ternary phase diagram of DNA, HA and water if no mixing is assumed. (b) Ternary phase diagram of DNA, HA and water if mixing of HA into DNA is assumed. A single-phase region is denoted as a triangle. Schematic representations of the sample volume are shown next to the respective diagrams, dark lines being HA chains and light ones, DNA.

In accordance with our initial assumption, there is no mixing of the phases and there is not a single phase region in the diagram. In the following, we question this assumption and suppose that a fraction of HA molecules ΔN_H mixes into the DNA phase (for brevity, we will use indices H for HA and D for DNA.). We remind that $N_H/V = c_H$ and that $N_H/V_H^\star = c_H^\star$.

Thus, the reduced concentration of pure HA phase, $c^{\star}_{H\Delta}$ would be:

$$c^{\star}_{H\Delta} = c^{\star}_{H} \times (1 - \Delta) \tag{7}$$

Also, from the above follows that the concentration of mixed-in HA fraction within the DNA subphase is $c^{\star}_{H\Delta} = \Delta N_H / V^{\star}_D$ which leads to:

$$c^{X}_{H\Delta} = \Delta \times c^{\star}_{D} \times (c_H / c_D) \tag{8}$$

Notably, it depends on the ratio of nominal (initial) concentrations of HA and DNA - more HA added, more mixing occurs. However, the Δ parameter still remains to be evaluated in order to define the phase diagram already presented in Figure 8b.

Osmotic pressure equilibrium and mixing

Towards this goal we continue by reminding that DNA and HA subphases are in the osmotic equilibrium regulated by counterions. That is, the osmotic pressure of the DNA subphase with a HA fraction mixed-in equals the pressure of the HA subphase:

$$\Pi^{\star}_{D} + \Pi^{X}_{H\Delta} = \Pi^{\star}_{H\Delta}. \tag{9}$$

The osmotic pressure for DNA as a highly charged PE is defined by the osmotic pressure coefficient $\phi_D = (2\eta_D)^{-1}$ (η is the Manning parameter, see Appendix) and the counterion concentration $2c^{\star}_{D}$ (there are two counterions per monomer-basepair):

$$\Pi^{\star}_{D} \propto 2\phi_D \times c^{\star}_{D} \tag{10}$$

The osmotic pressure for HA as a weakly charged PE is defined by the osmotic pressure coefficient $\phi_H = 1 - 0.5\eta_H = 0.64$ ($\eta_H = 0.72$ for HA) and the counterion concentration $c^{\star}_{H}$. We now equalize the osmotic pressures of the two subphases, taking into account the

possible intermixing, Eq. 8:

$$\phi_H c^{\star}_{H\Delta} = [2\phi_D + \Delta\phi_H \times (c_H/c_D)] \times c^{\star}_D \tag{11}$$

Now, we take into account the experimentally obtained relationship of effective concentrations of HA and DNA, Eq. 5, as well as Eq. 7 and get:

$$\Gamma\phi_H \times (1-\Delta) = 2\phi_D + \Delta\phi_H \times (c_H/c_D) \tag{12}$$

This expression is the condition for intermixing of HA into DNA subphase. The expression may be satisfied for different values of parameters Δ , c_H/c_D and only for $\phi_D \leq 0.28$, that is:

$$\Delta = (\Gamma - 2\phi_D/\phi_H)/(c_H/c_D + \Gamma) \tag{13}$$

If we take the theoretical values (see Appendx or [85]) of the osmotic coefficients for DNA, $\phi_D = 0.12$ and HA, $\phi_D = 0.65$ we get

$$\Delta = 0.47/(c_H/c_D + 0.87) \tag{14}$$

Thus we obtain the fraction of HA within the DNA phase:

$$c^{X}_{H\Delta}/c^{\star}_D = 0.47 \times \frac{(c_H/c_D)}{c_H/c_D + 0.87} \tag{15}$$

Interestingly, the higher the relative HA content, the higher the fraction of HA which should mix into DNA. For the lowest HA contents that we tested $c_{HA} < 0.1 \times c_{DNA}$ the ratio of HA and DNA in DNA domains would be $0.47 \cdot (0.1/0.95) \sim 5\%$ while it would rise to 45% for the highest HA contents $c_{HA} > 30 \times c_{DNA}$. It is debatable whether this could be considered physical. That is, the ternary phase diagram with mixing, Figure 8b) qualitatively differs from the one without the mixing, Figure 8a) as in the former appears

a single-phase mixture region which lacks in the latter. However, this region is broadening towards higher DNA or HA content, in contradiction with the case presented by Hellebust et al. where the single phase mixture occurs only at the lowest concentrations of PEs and disappears towards higher PE contents.[69]

Osmotic pressure equilibrium and Manning condensation parameter

Importantly, the expression Eq. 13 when there is no intermixing ($\Delta = 0$) may be satisfied only if an osmotic coefficient different from Manning theoretical value is assumed, that is $\phi_D = 0.28$, double the Manning value! Indeed, Raspaud et al. have found quite similar $\phi_D = 0.25$ also from a measurement of DNA osmotic pressure. That is, they have equilibrated DNA with neutral polymer PEG, while we did the equilibration with the charged polymer HA, a polyelectrolyte. While giving a similar value, the two approaches are quite different in a technical sense - as they used osmometry, while we use SAXS. More importantly - we use HA, a weakly charged PE which does not feature Manning condensation. Consequently, we have a good knowledge of the free counterion concentration and the osmotic coefficient in HA subphase and then its straight forward to equilibrate these with DNA subphase - as shown above. There is no need to have previously established the dependence of the osmotic pressure on the concentration of the stressing polymer - there are no issues related to calibration of osmometers etc. This adds confidence to the absolute numbers for osmotic coefficient $\phi_D = 0.28$ and the Manning parameter $f_D = 0.55$ that we obtain and strongly corroborates the result by Raspaud et al.

Finally, we compare the results on the osmotic pressure of DNA and PSS (polystyrene sulfonate) from literature, with our findings. Firstly, from the above we take that the value of the osmotic coefficient should be double the theoretical for both DNA and PSS, *i.e.*$2(2\eta)^{-1}$ instead of $(2\eta)^{-1}$. For HA the osmotic coefficient may be expected to remain at the theoretical value $\phi_H = 1 - 0.5\eta_H = 0.64$ as it's not related to condensation. Secondly, we note the proportionality of concentrations (Eq. 5) of DNA and HA in osmotic equilibrium. Here, it

follows that the HA osmotic pressure $\Pi_{HA}(c)$ scales as for the other two PEs, $\Pi \sim c^{9/8}$, up to about $c = 1$ M.[75] In Figure 9 we present the literature osmotic pressure data for DNA and PSS and compare it with our findings for HA. That is, for HA we infer the osmotic pressure from the fact that it is equilibrated with DNA $\Pi_{HA} = \Pi_{DNA}$ and from $c_{HA}^{monomer} = \Gamma \cdot c_{DNA}^{basepair}$. We remind that for DNA $c_{DNA}^{counterion} = 2c_{DNA}^{basepair}$.

$$\Pi_{DNA}/RT = \phi_{DNA} c_{DNA}^{counterion} = 2(2\eta_{DNA})^{-1} \cdot c_{DNA}^{base} = 0.25 c_{DNA}^{counterion} \tag{16}$$

$$\Pi_{HA}/RT = \phi_{HA} c_{HA}^{counterion} = (1 - 0.5\eta_{HA}) \cdot c_{HA}^{monomer} = 0.65 \cdot c_{HA}^{counterion} = 0.25 c_{DNA}^{counterion} \tag{17}$$

Also,

$$\Pi_{PSS}/RT = \phi_{PSS} c_{PSS}^{counterion} = 2(2\eta_{PSS})^{-1} \cdot c_{PSS}^{monomer} = 0.35 c_{PSS}^{counterion} \tag{18}$$

In the set of the Equations above we have omitted the 9/8 exponent over c for the reasons of clarity. That is, the prefactors of interest herar are independent of the exponent. Accordingly, in Figure 9 we plot on the x-axis the total counterion concentration $c_{counterion}$ of the PEs in question and the y-axis is the osmotic pressure rescaled by $RT\phi$ of the respective PE. We arrive at a single (experimental) master curve for DNA, HA and PSS. In other words, there is no other prefactor in the equation of state for all the PEs besides the osmotic pressure coefficient: $\Pi = \phi cRT$. On the contrary, if we take the Manning theoretical values of the osmotic coefficient then different PEs would feature different prefactors. In other words, we arrive to a master curve for Π if we take the condensation parameter to be double the Manning value - as also found by Raspaud et al. Eventually, this shows that in our DNA/HA mixture there is no intermixing and that the phase separation is complete.

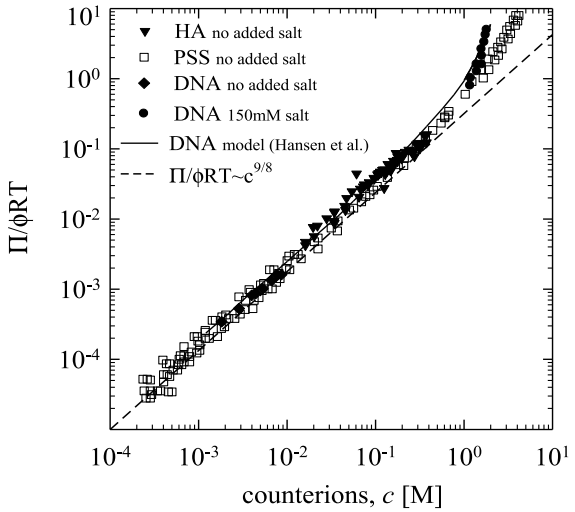

Figure 9: Equation of state for DNA, HA and PSS. The osmotic pressure is rescaled by the osmotic coefficient of a given PE, where the osmotic coefficient for strong PEs (DNA, PSS) is taken to be η^{-1}, *i.e.* double the Manning theoretical value $(2\eta)^{-1}$ and for HA is $1 - 0.5\eta$, (η is the Manning parameter for a given PE).

Conclusion and prospects

At the end we note the issue of the viscosity of the DNA and HA solutions, which depends on the size distribution of DNA and HA fragments in the sample. Our work was performed with solutions of long polydisperse 1-10 μm long DNA or HA molecules which are highly viscous, almost gel-like towards the highest concentrations. E.g., the global, flow induced anisotropy of the samples is preserved and visible in the SAXS anisotropy. Mixtures of DNA and HA consisting of shorter fragments, down to 0.1 μm would be much less viscous at similar concentrations. This could lead to different mixing properties, more akin to those for synthetic PEs tested by Hellebust et al. However, it is not *a priori* clear whether the phase separation or the homogenization will be facilitated by the diminished viscosity of the system. In other words, the phase separation that we observed could be a consequence of different electrostatic properties of DNA and HA and occur also for systems based on fragmented molecules, or it may be simply due to high viscosity and disappear when the viscosity is reduced. Of interest would also be whether more defined DNA mesophases (e.g. cholesteric) would be formed and how would the phase diagram compare to the one obtained

with the conventional PEG osmotic stressing method.

Acknowledgement

We gratefully acknowledge Elettra-Sincrotrone, Trieste for the beam-time. This work is primarily based on the support from the Unity through Knowledge Fund, Croatia under Grant 17/13 "Confined DNA" and also Grant 22/08. D. Grgičin and K. Salamon were also supported by grants from the Croatian Ministry of Science, Education and Sports.

Supporting Information Available

We provide the calibration relationship of the mesh size correlation length obtained by SAXS *vs.*DNA concentration. We also provide the evidence that the SAXS scattering peak for a given DNA concentration is not broadened by the presence of HA subdomains. Finally, we present an analysis of PLM images where the contents of birefringent, *i.e.* DNA and nonbirefringent, *i.e.* HA phase is quantitated. This information is available free of charge via the Internet at http://pubs.acs.org/.

Appendix

We summarize basic textbook concepts,[2,3] relevant for this work.

Persistence length – There are two charged elements in a PE system, polyions and the ionic cloud, and consequently there are electrostatics induced phenomena that are of primary concern in PE studies and repeatedly attract the attention of theoreticians and experimentalists[5–9,11–14] . One phenomenon is the electrostatic contribution L_e to the structural (intrinsic) persistence length L_0 (a measure of the polyion chain rigidity). That is, the persistence length $L_p = L_0 + L_e$ of a polyion is due to the structural rigidity of the constitutent polymer chain but also due to the long-range Coulomb repulsion of the like charges on the chain. It is inherently dependent on the screening of these charges by all the ions in the cloud (counterions and added-salt ions). A frequently used model to calculate L_e is Odijk-Skolnick-Fixman

model $L_e = 1/(4\kappa^2 l_B)$, where l_B is Bjerrum length. The electrostatic contribution may easily surpass the structural one in very low salt conditions. A polyion will behave as a rod if the persistence length is comparable to the contour length, $L_p \approx L_c$[86–90] .

Manning condensation – Manning condensation occurs for a polyion with a rather high linear charge density. Such a polyion is able to attract (condense), by long range Coulomb interaction, a fraction of the counterions released (by solvation) into the cloud. In simplest terms, Manning condensation occurs if the charges along the polyion are closer than the Bjerrum length, *i.e.*if their interaction is stronger than the thermal energy k_{BT}. E.g., for DNA, there are two charges per monomer ($z_m = 2$) and $b_{DNA} = 0.34$ nm which gives $\eta = z_m \times l_B/b = 4.2$ and $f = 1/\eta = 0.24$ Only 1 out of 4 counterions is uncondensed. On the other hand, HA has one charge per monomer ($z_m = 1$) of the length $b_{HA} = 1nm$,[91] which is longer than the Bjerrum length $l_B = 0.72$ nm. Thus, the Manning charge density parameter $\eta = 0.7$ for HA is smaller than 1 and its counterions do not Manning condense, $f = 1$.[7,85]

Osmotic pressure – One experimental parameter where nominally both the polyions and counterions come into play is the osmotic pressure.[9] In the limit of low salt concentrations, the osmotic pressure is proportional to the pressure from the ideal gas of (uncondensed) counterions, $\Pi_{ion} = \phi k_{BT} c$. The osmotic pressure coefficient is regulated by the Manning condensation for strong linear charge polyelectrolytes like DNA, $\eta > 1$: $\phi = (2\eta)^{-1}$. Low linear charge PE $\eta < 1$, like HA do not feature condensation but the osmotic coefficient is still below 1, as the screening effects due to the counterions are taken into account: $\phi_H = 1 - 0.5\eta_H = 0.64$.[85] Polyions also contribute to the osmotic pressure of PE. One way to describe a polyion is to take it as composed of rigid segments (Kuhn lengths). These are comparable to persistence length, L_p. Respective contribution to the osmotic pressure is $\Pi_{chain} = k_{BT}/L_p^3$. Nevertheless, L_p^3 will be smaller than ϕc at least up to $c = 0.5 - 1$M (monomers). Thus we'd have osmotic pressure proportional to the counterion concentration. However, experimentally, it occurs that the dependence is $\Pi \sim c^{9/8}$.[52,75] We may start here to note that this is observed for a semidilute solution, where polyions overlap. For such a

system we should take note of the scaling arguments for uncharged polymers first. There, the polymer size is the Flory radius which scales as $R_F \sim N^{3/5}$ (N = polymerization degree). The overlap concentration of separate chains scales as $c^\star \approx N/R_F^3$. The osmotic pressure Π of a semidilute system should not depend on N - the separate chains lose their identity in the semidilute regime. Thus, Π should be a function of only the monomer concentration: $\Pi = f(c/c^\star)$. Combining these expressions we get that $\Pi \sim (c/c^\star)^{9/4}$, as was confirmed experimentally.[75] Now, charged polymer (PE) in a high added salt environment should behave in a similar manner, as the screening reduces interchain interactions. However, effects of charge interactions along he chain should be taken into account. A measure for the interaction along the chain is the electrostatic persistence length L_e, which should be compared to the Debye screening length $\kappa^{-1} \sim c^{-1/2}$ that scales with the square-root of the ionic concentration. Odijk gave the osmotic pressure for a semidilute salt-free PE with $\Pi \sim (L_e/\kappa)^{3/4} c^{9/4}$. In the salt-free conditions both L_e and κ^{-1} are defined by counterion (or monomer) concentration. This expression reduces to $\Pi \sim c^{9/8}$, which is indeed observed experimentally for DNA.

References

(1) Raspaud, E.; da Conceiçao, M.; Livolant, F. *Phys. Rev. Lett.* **2000**, *84*, 2533.

(2) Rubinstein, M.; Colby, R. H. *Polymer Physics*; Oxford University Press:Oxford; UK, 2003.

(3) van der Maarel, J. R. C. *Introduction to Biopolymer Physics*; World Scientific; Singapore, 2007.

(4) Thomas, S.; Durand, D.; Chassenieux, C.; Jyotishkumar, P. *Handbook of Biopolymer-Based Materials: From Blends and Composites to Gels and Complex Networks*; John Wiley & Sons; 2013.

(5) Oosawa, F. *Polyelectrolytes*; Marcel Dekker; New York, 1971, Chap. 5.

(6) de Gennes, P.-G.; Pincus, P.; Velasco, R. M.; Brochard, F. *J. Phys. (Paris)* **1976**, *37*, 1461.

(7) Manning, G. S. *Quart. Rev. Biophys.* **1978**, *11*, 179.

(8) Odijk, T. *Macromolecules* **1979**, *12*, 804.

(9) Dobrynin, A. V.; Rubinstein, M. *Prog. Polym. Sci.* **2005**, *30*, 1049.

(10) Förster, S., Schmidt, M. *Adv. Polym. Sci.* **1995**, *120*, 53.

(11) Netz, R. R.; Andelman, D. *Physics Reports.* **2003**, *380*, 1-95.

(12) Andresen, K.; Qiu, X.; Pabit, S. A.; Lamb, J. S.; Park, H. Y.; Kwok, L. W.; Pollack, L. *Biophys. J.* **2008**, *95*, 287.

(13) Wong, G. C.; Pollack, L. *Annu. Rev. Phys. Chem.* **2010**, *61*, 171.

(14) Mazur, A. K.; Maaloum, M. *Phys. Rev. Lett.* **2014**, *112*, 068104.

(15) Sukhishvili, S. A.; Kharlampieva, E.; Izumrudov, V. *Macromolecules* **2006**, *39*, 8873.

(16) Branton, D.; Deamer, D. W.; Marziali, A.; Bayley, H.; Benner, S. A.; Butler, T.; Di Ventra, M.; Garaj, S.; Hibbs, A.; Huang, X.; Jovanovich, S. B.; Krstic, P. S.; Lindsay, S.; Ling, X. S.; Mastrangelo, C. H.; Meller, A.; Oliver, J. S.; Pershin, Y. V.; Ramsey,J. M.; Riehn, R.; Soni, G. V.; Tabard-Cossa, V.; Wanunu, M.; Wiggin, M.; Schloss J. A. *Nature Biotechnology* **2008**, *26*, 1146.

(17) Buxboim, A.; Daube, S. S.; Bar-Ziv, R. *Nano Lett.* **2009**, *9*, 909.

(18) Brachaa, D.; Karzbruna, E.; Shemera, G.; Pincus, P. A.; Bar-Ziv, R. *PNAS* **2013**, *110*, 4534.

(19) Ewert, K. K.; Zidovska, A.; Ahmad, A.; Bouxsein, N. F.; Evans, H. M.; McAllister, C. S.; Samuel, C. E.; Safinya C. R. *Top Curr. Chem.* **2010**, *296*, 191.

(20) Jianhao, B.; Sebastian, B.; Yein, T. S.; Dieter, T.; *ACS Appl. Mater. Interfaces* **2011**, *3*, 1665.

(21) Merchant, C. A.; Drndić, M.; *Methods Mol. Biol.* **2012**, *870*, 211.

(22) Akabayov, B., Akabayov, S. R., Lee, S.-J., Wagner, G., Richardson, C. C. *Nature Comm.* **2013**, *4*, 1615.

(23) Elcock, A. H. *Curr. Opin. Struct. Biol.* **2010**, *20*, 196.

(24) Wang, Q.; Liang, K.-C.; Czader, A.; Waxham, M. N.; Cheung, M. S. *PLoS Comput. Biol.* **2011**, *7*, e1002114.

(25) Schmit, J. D.; Kamber, E.; Kondev, J.; *Phys. Rev. Lett.* **2009**, *102*, 218302.

(26) Krotova, M. K.; Vasilevskaya, V. V.; Makita, N.; Yoshikawa, K.; Khokhlov, A. R. *Phys. Rev. Lett.* **2010**, *105*, 128302.

(27) Lee, G. M.; Johnstone, B.; Jacobson, K.; Caterson, B. J. *Cell. Biol.* **1993**, *123*, 899-907.

(28) Evanko, S. P.; Tammi, M. I.; Tammi, R. H.; Wight, T. N. *Adv. Drug Deliv. Rev.* **2007**, *59*, 1351-65.

(29) Horkay, F. *J. Polym. Sci. B Polym. Phys.* **2012** *50*, 1699-1705.

(30) *Essentials of Glycobiology. 2nd edition.* Varki, A.; Cummings, R. D.; Esko, J. D.; Freeze, H. H.; Stanley, P.; Bertozzi, C. R.; Hart, G. W.; Etzler, M. E., editors. Cold Spring Harbor (NY): Cold Spring Harbor Laboratory Press; 2009.

(31) Hamley, I. W. *Soft Matter* **2010**, *6*, 1863-1871.

(32) Rill, R. L. *Proc. Natl. Acad. Sci. USA* **1986**, *83*, 342-6.

(33) Livolant, F.; *J. Physique* **1987**, *48*, 1051.

(34) Livolant, F.; Levelut, A. M.;Doucet, J.; Benoit, J. P.; *Nature* **1989**, *339*, 724-726.

(35) Strzelecka, T. E.; Rill, R. L. *Biopolymers* **1990**, *30*, 57-71.

(36) Livolant, F.; Leforestier, A. *Prog. Polym. Sci.* **1996**, *21*, 1115-1164.

(37) Merchant, K.; Rill, R. L. *Macromolecules* **1994**, *27*, 2365-2370.

(38) Merchant, K.; Rill, R. L. *Biophys J.* **1997**, *73* 3154-3163.

(39) Auer, H. E.; Alexandrowicz, Z.; *Biopolymers* **1969**, *8*, 1.

(40) Lerman, L. S. *Proc. Natl. Acad. Sci. USA* **1971**, *68*, 1886-1890.

(41) Vasilevskaya, V. V.; Khokhlov, A. R.; Matsuzawa, Y.;Yoshikawa, K. *J. Chem. Phys.* **1995**, *102*, 6595.

(42) Maniatis, T.; Venable, J. H.; Lerman, L. S. *Journal of Molecular Biology* **1974**, *84*, 37-64.

(43) Sikorav, J.-L.; Pelta, J.; Livolant, F. *Biophys. J.* **1994**, *67*, 1387.

(44) Raspaud, E.; de la Cruz, M. O.; Sikorav, J.-L.; Livolant, F. *Biophys. J.* **1998**, *74*, 381-393.

(45) Saminathan, M.; Thomas, T.; Shirahata, A.; Pillai, C. K. S.; Thomas, T. J. *Nucl. Acids Res.* **2002**, *30*, 3722-3731.

(46) Qiu, X,; Andresen, K.; Lamb, J. S.; Kwok, L. W.; Pollack, L. *Phys. Rev. Lett.* **2008**, *101*, 228101.

(47) Gelbart, W. M.; Bruinsma, R. F.; Pincus, P. A.; Parsegian, V. A. *Phys. Today* **2000**, *53*, 38.

(48) Zhang, R.; Shklovskii, B. I.; *Physica A* **2005**, *352*, 216-238.

(49) Tang, J. X.; Janmey, P. A.; *J. Biol. Chem.* **1996**, *271*, 8556-8563.

(50) Angelini, T. E.; Golestanian, R.; Coridan, R. H.; Butler, J. C.; Beraud, A.; Krisch, M.; Sinn, H.; Schweizer, K. S.; Wong, G. C. L. *Proc. Natl. Acad. Sci. USA* **2006**, *103*, 7962-7967.

(51) de Vries, R. *Biophys. J.* **2001**, *80*, 1186-1194.

(52) Hansen, P. L.; Podgornik, R.; Parsegian, V. A. *Phys. Rev. E* **2001**, *64*, 021907.

(53) Strey, H. H.; Parsegian, V. A.; Podgornik, R. *Phys. Rev. Lett.* **1997**, *78*, 895-898.

(54) Horkay, F.; Hecht, A.-M.; Geissler, E. *J. Polym. Sci. B Polym. Phys.* **2006** *44*, 3679-3686.

(55) Horkay, F.; Hecht, A.-M.; Rochas, .; Basser, P. J.; Geissler, E. *J. Chem. Phys.* **2006** *125*, 234904.

(56) Horkay, F.; Basser, P. J.; Londono, D. J.; Hecht, A.-M.; Geissler, E. *J. Chem. Phys.* **2009** *131*, 184902.

(57) Cleland, R. L. *Archives of Biochemistry and Biophysics* **1977** *180*, 57-68.

(58) Ribitsch, G.; Schurz, J.; Ribitsch, V. *Colloid and Polymer Science* **1980** *258*, 1322-1334.

(59) Villetti, M.; Borsali, R.; Diat, O.; Soldi, V.; Fukada, K. *Macromolecules* **2000** *33*, 9418.

(60) Cowman, M.K.; Matsuoka, S. *Carbohydr. Res.* **2005**, *340*, 791.

(61) Whistler, R. L.; Olson, E. J. *Advances in Carbohydrate Chemistry* **1957** *12*, 299-319.

(62) Adams, G. W.; Cowie, J. M. G. *Polymer* **1999**, *40*, 1993-2001.

(63) Zribi, O. V.; Kyung, H.; Golestanian, R.; Liverpool, T. B.; Wong, G. C. *Phys. Rev. E* **2006**, *73*, 031911.

(64) Lai, G. H.; Butler, J. C.; Zribi, O. V.; Smalyukh, I. I.; Angelini, T. E.; Purdy, K. R.; Golestanian, R.; Wong, G. C. L. *Phys. Rev. Lett.* **2008**, *101*, 218303.

(65) Flory, P. J. *Macromolecules* **1978**, *11*, 1138-1141.

(66) Khokhlov, A. R.; Nyrkova, I. A. *Macromolecules* **1992**, *25*, 1493.

(67) Li, X.; Denn, M. M. *Macromolecules* **2002**, *35*, 6446-6454.

(68) Picullel, L.; Nilsson, S.; Falck, L.; Tjerneld, F. *Polymer comm.* **1991**, *32*, 159.

(69) Hellebust, S.; Nilsson, S.; Blokhus, A. M. *Macromolecules* **2003**, *36*, 5372-5382.

(70) Moulton, S. E.; Maugey, M.; Poulin, P.; Wallace, G. G. *J. Am. Chem. Soc.* **2007**, *129*, p9452-7.

(71) Rau, D. C.; Lee, B. K.; Parsegian, V. A. *Proc. Natl. Acad. Sci. USA* **1984**, *81*, 2621.

(72) Podgornik, R.; Rau, D. C.; Parsegian, V. A. *Macromolecules* **1989**, *22*, 1780-1786.

(73) Salamon, K.; Aumiler, D.; Pabst, G.; Vuletić, T. *Macromolecules* **2013**, *46*, 1107.

(74) Wang, L.; Bloomfield, V. A. *Macromolecules* **1991**, *24*, 5791-5795.

(75) Wang, L.; Bloomfield, V. A. *Macromolecules* **1990**, *23*, 804-809.,

(76) Tomić, S.; Vuletić, T.; Dolanski Babić, S.; Krča, S.; Ivanković, D.; Griparić, L.; Podgornik R. *Phys. Rev. Lett.* **2006**, *97* 098303

(77) Tomić, S.; Dolanski Babić, S.; Vuletić, T.; Krča, S.; Ivanković, D.; Griparić, L.; Podgornik, R. *Phys. Rev. E* **2007**, *75*, 021905.

(78) Vuletić, T.; Dolanski Babić, S.; Ivek, T.; Grgičin, D.; Tomić, S.; Podgornik, R. *Phys. Rev. E* **2010**, *82*, 011922.

(79) Tomić, S.; Dolanski Babić, S.; Ivek, T.; Vuletić, T.; Krča, S.; Livolant, F.; Podgornik, R. *Europhys. Lett.* **2008**, *81*, 68003.

(80) Kaji, K.; Urakawa, H.; Kanaya, T.; Kitamaru, R. *J. Phys. (France)* **1988**, *49*, 993.

(81) Ito, K.; Yagi, A.; Ookubo, N.; Hayakawa, R. *Macromolecules* **1990**, *23*, 857.

(82) Amenitsch, H.; Rappolt, M.; Kriechbaum, M.; Mio, H.; Laggner, P.; Bernstorff, S.; *J. Synchrotron Radiat.* **1998**, *5*, 506-508.

(83) Wang, Z.-G.; Xia, Z.-Y.; Yu, Z.-Q.; Chen, E.-Q.; Sue, H.-J.; Han, C. C.; Hsiao, B. S.*Macromolecules* **2006**, *39*, 2930.

(84) Combet, J.; Isel, F.; Raviso, M.; Boue, F.*Macromolecules* **2005**, *38*, 7456.

(85) Manning, G. S. *J. Chem. Phys.* **1969**, *51*, 924.

(86) Odijk, T. *J. Polym. Sci. Polym. Phys. Ed.* **1977**, *15*, 477.

(87) Skolnick, J.; Fixman, M. *Macromolecules* **1977**, *10*, 944.

(88) Odijk, T. *Macromolecules* **1979**, *12*, 688.

(89) Baumann, C. G.; Smith, S. B.; Bloomfield, V. A.; Bustamante, C. *Proc. Natl. Acad. Sci. USA* **1997**, *94*, 6185.

(90) Ullner, M. *J. Chem. Phys.* **2003**, *107*, 8097.

(91) Buhler, E.; Boue, F. *Macromolecules* **2004**, *37*, 1600.

For Table of Contents Use Only

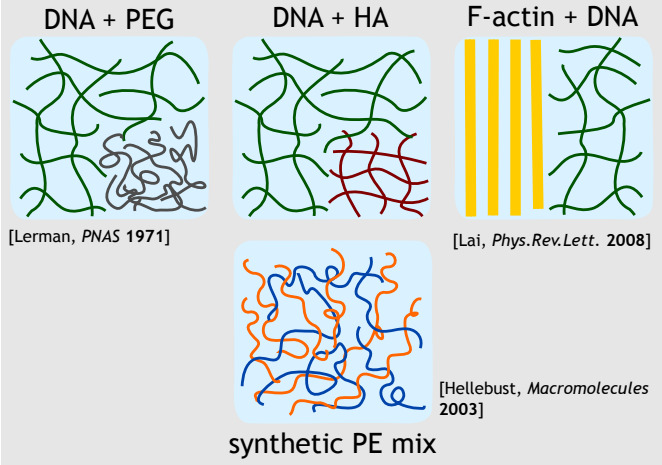

Table of Contents Graphic

Title: Polyelectrolyte composite: Hyaluronic acid mixture with DNA

Authors: I. Delač Marion, D. Grgičin, K. Salamon, S. Bernstorff, , and T. Vuletić